

Structure and stability of copper clusters: A tight-binding molecular dynamics study

Mukul Kabir* and Abhijit Mookerjee†

S. N. Bose National Centre for Basic Sciences, JD Block, Sector III, Salt Lake City, Kolkata 700098, India

A. K. Bhattacharya

Department of Engineering, University of Warwick, Coventry CV47AL, United Kingdom

(Received 7 November 2003; published 16 April 2004)

In this paper we propose a tight-binding molecular dynamics with parameters fitted to first-principles calculations on the smaller clusters and with an environment correction, to be a powerful technique for studying large transition-metal/noble-metal clusters. In particular, the structure and stability of Cu_n clusters for $n = 3-55$ are studied by using this technique. The results for small Cu_n clusters ($n = 3-9$) show good agreement with *ab initio* calculations and available experimental results. In the size range $10 \leq n \leq 55$ most of the clusters adopt icosahedral structure which can be derived from the 13-atom icosahedron, the polyicosahedral 19-, 23-, and 26-atom clusters, and the 55-atom icosahedron, by adding or removing atoms. However, a local geometrical change from icosahedral to decahedral structure is observed for $n = 40-44$ and return to the icosahedral growth pattern is found at $n = 45$ which continues. Electronic “magic numbers” ($n = 2, 8, 20, 34, 40$) in this regime are correctly reproduced. Due to electron pairing in highest occupied molecular orbitals (HOMOs), even-odd alternation is found. A sudden loss of even-odd alternation in second difference of cluster binding energy, HOMO-LUMO (LUMO, lowest unoccupied molecular orbital) gap energy and ionization potential is observed in the region $n \sim 40$ due to structural change there. Interplay between electronic and geometrical structure is found.

DOI: 10.1103/PhysRevA.69.043203

PACS number(s): 36.40.Cg, 36.40.Mr, 36.40.Qv

I. INTRODUCTION

The study of clusters has become an increasingly interesting topic of research in both physics and chemistry in recent years, since they span the gap between the microscopic and macroscopic materials [1,2]. Metallic clusters play a central role in catalysis [3–6] and nanotechnology [7–9]. Clusters of coinage metals Cu, Ag, and Au have been used in a wide range of demonstration [3–9]. The determination of structural and electronic properties and the growth pattern of coinage metal clusters are of much interest both experimentally [10–18] and theoretically [19–24]. The electronic configurations of the coinage metals are characterized by a closed d shell and a single s valance electron [$\text{Cu}:\text{Ar}(3d)^{10}(4s)^1$, $\text{Ag}:\text{Kr}(4d)^{10}(5s)^1$, $\text{Au}:\text{Xe}(5d)^{10}(6s)^1$]. Due to the presence of single s electrons in the atomic outer shells, the noble-metal clusters are expected to exhibit certain similarities to the alkali-metal clusters. Electronic structure of alkali-metal clusters is well described by the spherical shell model, which has successfully interpreted the “magic numbers” in Na_n and K_n clusters [1,2]. A number of experimental features of noble-metal clusters are also qualitatively well described in terms of simple s electron shell model. For instance, the mass abundance spectrum of Cu_n^- , Ag_n^- , and Au_n^- clusters, which reflects the stability of clusters, can be explained by the one-electron shell model [10]. But some experimental studies [11–14] indicate that the localized d electrons of the noble metals play a significant role for the

geometrical and electronic structure through the hybridization with more extended valence s electron. Therefore, it is important to include the contribution of $3d$ electrons and the s - d hybridization for Cu_n clusters.

Bare copper clusters in the gas phase have been studied experimentally by Taylor *et al.* [15] and Ho *et al.* [16] using photoelectron spectroscopy (PES). Knickelbein measured ionization potentials of neutral copper clusters and found evidence of electronic shell structure [17]. Very recently, cationic copper clusters have been studied using threshold collision-induced dissociation (TCID) by Spasov *et al.* [18]. Copper clusters have been also investigated theoretically by various accurate quantum-mechanical and chemical approaches. Massobrio *et al.* [19] studied the structures and energetics of Cu_n ($n = 2, 3, 4, 6, 8, 10$) within the local-density approximation of density-functional theory (DF-LDA) by using the Car-Parinello method. Calaminici *et al.* [20] used the linear combination of Gaussian-type orbitals density functional approach to study Cu_n , Cu_n^- , and Cu_n^+ clusters with $n \leq 5$. Akeby *et al.* [21] used the configuration interaction method with an effective core potential for $n \leq 10$. In an earlier communication [22] we studied the small Cu_n clusters for $n \leq 9$ by using full-potential muffin-tin orbitals (FP-LMTO) technique.

Ideally, the sophisticated, quantum-chemistry-based, first-principles methods predict both the stable geometries and energetics to a very high degree of accuracy. The practical problem arises from the fact that for actual implementation these techniques are limited to small clusters only. None of the methods described above can be implemented for clusters much larger than ~ 10 atoms, because of prohibitive computational expense. The aim of this paper is to introduce an semiempirical method, which, nevertheless, retains some

*Corresponding author. Email address: mukul@bose.res.in

†Email address: abhijit@bose.res.in

of the electronic structure features of the problem. The empirical parameters are determined from first-principles calculations for small clusters, and corrections introduced for local environmental corrections in the larger clusters.

In recent years empirical tight-binding molecular dynamics (TBMD) method has been developed as an alternative to *ab initio* methods. As compared with *ab initio* methods, the parametrized tight-binding Hamiltonian reduces the computational cost dramatically. The main problem with the empirical tight-binding methods has always been the lack of transferability of its empirical parameters. We shall describe here a technique that allows us to fit the parameters of the model from a fully *ab initio*, self-consistent local spin-density approximation based FP-LMTO calculation reported earlier by us [22,23] for the smaller clusters and then make correction for the new environment for clusters in order to ensure transferability (at least to a degree).

It should be mentioned here that copper clusters have also been investigated by other empirical methods. D'Agostino carried out molecular dynamics using a quasiempirical potential derived from a tight-binding approach for nearly 1300 atoms [24]. More recently, Darby *et al.* carried out geometry optimization by genetic algorithm using Gupta potential [25] for Cu_n , Au_n , and their alloy clusters in the size range $n \leq 56$ [26]. These kinds of empirical atomistic potentials are found to be good to predict ground-state geometries but cannot predict electronic properties such as electronic shell closing effect for $n=2, 8, 20, 40, \dots$, highest occupied–lowest unoccupied molecular level (HOMO-LUMO) gap energy and ionization potential. Our proposed TBMD scheme will allow us to extrapolate to the larger clusters to study both the ground-state geometries as well as ground-state energetics as a function of cluster size.

Menon *et al.* have proposed a minimal parameter TBMD scheme for semiconductors [27–29] and extended the method for transition-metal (Ni_n and Fe_n) clusters [30,31]. Recently Zhao *et al.* have applied this method for silver clusters [32]. In the present work, we shall introduce a similar TB model for copper.

Using this TBMD method, we shall investigate the stable structures, cohesive energies, relative stabilities, HOMO-LUMO gaps, and ionization potentials of Cu_n clusters in the size range $n \leq 55$. We shall indicate the comparison between the present results for small clusters, $n \leq 9$, with those of our previous FP-LMTO calculations and other *ab initio* and available experimental results. This is essential before we go over to the computationally expensive study of larger clusters.

II. COMPUTATIONAL METHOD

Menon *et al.* introduced a minimal parameter TBMD scheme for transition-metal clusters [30,31]. Here we will describe the main ingredients. In this tight-binding scheme the total energy E is written as a sum,

$$E = E_{el} + E_{rep} + E_{bond}. \quad (1)$$

E_{el} is the sum of the one-electron energies for the occupied states ϵ_k ,

$$E_{el} = \sum_k^{occ} \epsilon_k, \quad (2)$$

where the energy eigenvalues ϵ_k are calculated by solving the eigenvalue equation

$$H|\Psi_k\rangle = \epsilon_k|\Psi_k\rangle, \quad (3)$$

where H is the one-electron Hamiltonian and $|\Psi_k\rangle$ is electronic wave function for k th level of the eigenstate. In the TB formulation, the single-particle wave functions $|\Psi_k\rangle$ are cast as a linear combination of orthogonalized basis functions $\Phi_{i\nu}$, in the minimum basis set ($\nu = s, p_x, p_y, p_z, d_{xy}, d_{yz}, d_{zx}, d_{x^2-y^2}, d_{3z^2-r^2}$),

$$|\Psi_k\rangle = \sum_{i\nu} c_{i\nu}^k |\Phi_{i\nu}\rangle, \quad (4)$$

where i labels the ions.

The TB Hamiltonian H is constructed within Slater-Koster scheme [33], where the diagonal matrix elements are taken to be configuration independent and the off-diagonal matrix elements are taken to have Slater-Koster type angular dependence with respect to the interatomic separation vector \mathbf{r} and scaled exponentially with the interatomic separation r :

$$V_{\lambda,\lambda',\mu} = V_{\lambda,\lambda',\mu}(d)S(l,m,n)\exp[-\alpha(r-d)], \quad (5)$$

where d is the equilibrium bond length for the fcc bulk copper, $S(l,m,n)$ is the Slater-Koster type function of the direction cosines l, m, n of the separation vector \mathbf{r} , and α is an adjustable parameter ($=2/d$) [31].

The Hamiltonian parameters are determined from the dimensionless universal parameters $\eta_{\lambda,\lambda',\mu}$ [34],

$$V_{\lambda,\lambda',\mu}(d) = \eta_{\lambda,\lambda',\mu} \left(\frac{\hbar^2 r_d^\tau}{m d^{\tau+2}} \right), \quad (6)$$

where r_d is characteristic length for the transition metal and the parameter $\tau=0$ for s - s , s - p , and p - p interactions, $\tau=3/2$ for s - d and p - d interactions, and $\tau=3$ for d - d interaction. In Table I we present the parameter r_d , the on-site energies E_s, E_p, E_d , and the universal constants $\eta_{\lambda,\lambda',\mu}$ for Cu [34]. According to Ref. [30,31], we set $E_s=E_d$ and E_p large enough to prevent p -orbital mixing [34]. This choice of our tight-binding parameters reproduces the band structure of the fcc bulk Cu crystal given by Harrison [34].

The repulsive energy E_{rep} is described by a sum of short-ranged repulsive pair potentials, ϕ_{ij} , which scaled exponentially with interatomic distance,

$$E_{rep} = \sum_i \sum_{j(>i)} \phi_{ij}(r_{ij}) = \sum_i \sum_{j(>i)} \phi_0 \exp[-\beta(r_{ij}-d)], \quad (7)$$

where r_{ij} is the separation between the atoms i and j and β ($=4\alpha$) is a parameter. E_{rep} contains ion-ion repulsive interaction and correction to the double counting of the electron-electron repulsion present in E_{el} . The value of ϕ_0 fitted to reproduce the correct experimental bond length of the Cu dimer, 2.22 Å [35], is given in Table II.

TABLE I. Parameter r_d , on-site energies, E_s , E_p , and E_d , and the universal constants $\eta_{\lambda,\lambda',\mu}$ for Cu [34].

Parameter	Value
r_d	0.67 Å
E_s	-20.14 eV
E_p	100.00 eV
E_d	-20.14 eV
$\eta_{ss\sigma}$	-0.48
$\eta_{sp\sigma}$	1.84
$\eta_{pp\sigma}$	3.24
$\eta_{pp\pi}$	-0.81
$\eta_{sd\sigma}$	-3.16
$\eta_{pd\sigma}$	-2.95
$\eta_{pd\pi}$	1.36
$\eta_{dd\sigma}$	-16.20
$\eta_{dd\pi}$	8.75
$\eta_{dd\delta}$	0.00

The first two terms of the total energy are not sufficient to exactly reproduce cohesive energies of dimers through bulk structures. Tomaňek and Schluter [36] introduced a coordination dependent correction term, E_{bond} , to the total energy, which does not contribute to the force, it is added to the total energy after the relaxation has been achieved. However, for the metal clusters, this correction term is significant in distinguishing various isomers for a given cluster [31].

$$E_{bond} = -n \left[a \left(\frac{n_b}{n} \right)^2 + b \left(\frac{n_b}{n} \right) + c \right], \quad (8)$$

where n and n_b are the number of atoms and total number of bonds of the cluster, respectively. Number of bonds n_b are evaluated by summing over all bonds according to cutoff distance r_c and bond length

$$n_b = \sum_i \left[\exp \left(\frac{r_{ij} - r_c}{\Delta} \right) + 1 \right]^{-1}. \quad (9)$$

The parameters a , b , and c in Eq. (6) are then calculated by fitting the coordination dependent term, E_{bond} , to the *ab initio* results for three small clusters of different sizes according to the following equation:

$$E_{bond} = E_{ab \text{ initio}} - E_{el} - E_{rep}. \quad (10)$$

Thus we have four parameters ϕ_0 , a , b , and c in this TB model. These parameters are once calculated (given in the Table II) for small clusters to reproduce known results (whatever experimental or theoretical) and then kept fixed for

TABLE II. The adjustable parameters ϕ_0 , a , b , and c .

ϕ_0 (eV)	a (eV)	b (eV)	c (eV)
0.034	-0.0671	1.2375	-3.0420

other arbitrary size cluster. To determine the parameters a , b , and c we use the experimental binding energy of Cu dimer 1.03 eV/atom [35] and the *ab initio* FP-LMTO results for Cu₄ and Cu₆ in Ref. [22]. For the Cu₂ dimer, calculated vibrational frequency (226 cm⁻¹) has reasonable agreement with experiment [37] (265 cm⁻¹).

In molecular dynamics scheme the trajectories $\{\mathbf{R}_j(t)\}$ of the ions are determined by the potential energy surface $E[\{\mathbf{R}_j(t)\}]$ corresponding to the total energy of the electronic system. The force acting on the i th ion is thus given by

$$\mathbf{F}_i = -\nabla_{\mathbf{R}_i} E[\{\mathbf{R}_j\}] = -\nabla_{\mathbf{R}_i} \left[\sum_k \langle \Psi_k | H | \Psi_k \rangle + E_{rep} \right]. \quad (11)$$

This equation can be further simplified by making use of the Hellmann-Feynman [38] theorem

$$\mathbf{F}_i = -\sum_k \langle \Psi_k | \nabla_{\mathbf{R}_i} H | \Psi_k \rangle - \nabla_{\mathbf{R}_i} E_{rep}. \quad (12)$$

The second term in the above equation is the short-ranged repulsive force. We should note that Pulay correction term does not play any role in any semiempirical TBMD [39]. The reason is twofold. Within TBMD we directly compute the derivative of the TB Hamiltonian matrix element and the basis wave functions never appear explicitly, rather they are implicitly contained in the fitted matrix entries.

The motion of the atoms follows a classical behavior and is governed by the Newton's law,

$$m \frac{d^2 \mathbf{R}_i}{dt^2} = \mathbf{F}_i, \quad (13)$$

where m is the atomic mass.

For numerical simulation of Newtonian dynamics, we use the velocity Verlet molecular dynamics method [40] for updating the atomic coordinates, which is given by

$$\mathbf{R}_i(t + \delta t) = \mathbf{R}_i(t) + \mathbf{V}_i(t) \delta t + \frac{1}{2m} \mathbf{F}_i(t) (\delta t)^2, \quad (14)$$

where the velocity \mathbf{V}_i of the i th atom at $t + \delta t$ is calculated from \mathbf{F}_i at t and $t + \delta t$ as

$$\mathbf{V}_i(t + \delta t) = \mathbf{V}_i(t) + \frac{1}{2m} [\mathbf{F}_i(t) + \mathbf{F}_i(t + \delta t)] \delta t. \quad (15)$$

At this stage most authors carry out either dissipative dynamics or free dynamics with feedback [41]. The reason for this is as follows: for numerical integration of Newton's equations we have to choose a *finite* time step δt . Ideally this should be as small as possible, but that would require an excessively long time for locating the global minimum. However, a large choice of δt leads to unphysical heating up of the system, leading to instability. Dissipative dynamics has been suggested as a way of overcoming this. We add a small extra friction term carefully, $\mathbf{F} \Rightarrow \mathbf{F} - \gamma m \dot{\mathbf{R}}$ [31]. In the present calculation $\gamma m = 0.32$ amu/psec, and the time step δt is taken to be 1 fsec and the total time for molecular dynamics simulation is ~ 100 – 200 psec, depending upon the cluster size and initial cluster configuration with the several annealing schedule. Methfessel and Schilfgaarde [41] have also

TABLE III. Point group (PG) symmetry, cohesive energy per atom, difference in cohesive energy per atom ΔE , and average bond length $\langle r \rangle$ of the ground-state structure and different isomers for Cu_n clusters with $n \leq 9$ obtained from TB calculation and comparison with *ab initio* calculations [19,21,22]. $\Delta E=0.00$ represents the most stable structure for a particular n . Cohesive energy corresponding to the ground-state structure in FP-LMTO [22], DF-LDA [19] (in parentheses) calculations and the values from TCID experiment [18] are given. For Cu_7 , $C_{3v}(\text{I})$ is the bicapped trigonal bipyramid and $C_{3v}(\text{II})$ is the capped octahedron.

Cluster	PG symmetry	Binding energy (eV/atom)			ΔE (eV/atom)			$\langle r \rangle$ (Å)
		Present	Theory ^a	Experiment ^b	Present	Theory ^c	Theory ^d	
Cu_3	C_{2v}	1.43	1.60(1.63)	1.07 ± 0.12	0.00		0.00	2.25
	D_{3h}	1.32			0.11	0.06		2.24
	$D_{\infty h}$	1.13			0.30	0.00		2.24
Cu_4	D_{2h}	2.00	2.00(2.09)	1.48 ± 0.14	0.00	0.00	0.00	2.23
	D_{4h}	1.73			0.27	0.56		2.22
	T_d	1.46			0.54	0.89		2.24
Cu_5	C_{2v}	2.24	2.19	1.56 ± 0.15	0.00	0.00		2.23
	D_{3h}	2.03			0.21	0.37		2.38
Cu_6	C_{5v}	2.54	2.40(2.49)	1.73 ± 0.18	0.00	0.00	0.00	2.40
	C_{2v}	2.40			0.14		0.01	2.39
	O_h	1.98			0.56	0.87	0.04	2.41
Cu_7	D_{5h}	2.63	2.65	1.86 ± 0.22	0.00	0.00		2.41
	$C_{3v}(\text{I})$	2.50			0.13	0.32		2.63
	$C_{3v}(\text{II})$	2.30			0.33			2.45
Cu_8	C_s	2.87	2.73(2.84)	2.00 ± 0.23	0.00		0.20	2.41
	O_h	2.64			0.23			2.61
	D_{2d}	2.57			0.30		0.00	2.59
	T_d	2.51			0.36		0.15	2.39
Cu_9	C_2	2.87	2.80		0.00			2.44
	C_{2v}	2.84			0.03			2.59
	C_s	2.60			0.27			2.41

^aFrom Kabir *et al.* (Ref. [22]) and Massobrio *et al.* (Ref. [19]).

^bCalculated from Spasov *et al.* (Ref. [18]).

^cFrom Akeby *et al.* (Ref. [21]).

^dFrom Massobrio *et al.* (Ref. [19]).

used an alternative technique of free dynamics with feedback to overcome the above difficulty.

The results of the molecular dynamics may depend sensitively on the starting configuration chosen. The final equilibrium configurations often correspond to local minima of the total energy surface and are metastable states. For the smaller clusters simulated annealing can lead to the global minimum. We have found the global minimum configurations of the smaller clusters by the simulated annealing technique. However, this is often not the case for the larger clusters. Recently more sophisticated techniques such as the genetic algorithm have been proposed [42–45]. We have not tried this out in this work, but propose this as an efficient technique for further work.

III. RESULTS AND DISCUSSION

A. Geometry optimization

We have applied this TBMD scheme to Cu_n clusters for $n \leq 55$. Since the present scheme imposes no *a priori* symmetry restrictions, we can perform full optimization of clus-

ter geometries. For small clusters ($n \leq 9$) we can perform a full configurational space search to determine the lowest-energy configuration. Here they serve as a test case for the calculation of larger clusters with $n \geq 10$. In Table III we present a detailed comparison of binding energy per atom, difference in binding energy ΔE , and average bond length $\langle r \rangle$ for $n \leq 9$ with available experimental [18] and *ab initio* [19,21,22] results. We found that, in agreement with experimental [16] and theoretical [19–21] results, very small copper clusters (Cu_3 , Cu_4 , and Cu_5) prefer planar structures. More detailed comparison, with experimental and *ab initio* results, can be found elsewhere [46].

From the present results and detailed comparisons with various experimental [16,18] and *ab initio* [19–22,47–49] results available, we find reasonable agreement among this TBMD scheme and *ab initio* calculations for small clusters with $n \leq 9$ [46], which allow us to continue the use of this TBMD scheme for larger clusters with $n \geq 10$. For larger clusters ($10 \leq n \leq 55$), due to increasing degrees of freedom with cluster size, a full configurational search is not possible with the available computational resources. Instead, led by the experimental and theoretical results on small clusters, we

examined structures of various symmetries for each size. Most stable structures for $n=10-55$ atom clusters are given in Fig. 1.

In this regime, the structures predicted by this TB model are mainly based on icosahedron. The most stable structure of Cu_7 is a pentagonal bipyramid (D_{5h} symmetry; see Table III), which is the building block for the larger clusters with $n \geq 10$. For Cu_{10} , we found a tricapped pentagonal bipyramid to be the most stable structure. Ground-state structures of Cu_{11} and Cu_{12} are the uncompleted icosahedron with lack of one and two atoms, respectively, and a Jahn-Teller distorted *first* complete icosahedron is formed at Cu_{13} . For Cu_{13} , the fcc like cuboctahedron is less stable than the icosahedron by an energy 0.05 eV per atom. In agreement with Lammers and Borstel, on the basis of tight-binding linear muffin-tin orbital calculations, was also found the icosahedron to be the ground state of Cu_{13} , though the difference in energy between the icosahedron and the cuboctahedron was calculated to be only 0.2 eV/atom [48]. The ground-state structures for Cu_{14} , Cu_{15} , Cu_{16} , and Cu_{17} are the 13-atom icosahedron plus one, two, three, and four atoms, respectively. A double icosahedron is formed for Cu_{19} (D_{5h} symmetry). This structure has two internal atoms, 12 six-coordinate atoms at either end, and five eight-coordinate atoms around the waist of the cluster. Based on the structure for Cu_{19} , the stable Cu_{18} cluster is a double icosahedron minus one of the six-coordinate atoms located at either end (C_{5v} symmetry). Icosahedral growth continues for $20 \leq n \leq 55$ atom clusters. Polyicosahedral structure in the form of a “triple icosahedron” (D_{3h} symmetry; the structure can be viewed as three interpenetrating double icosahedra) is the most stable structure for Cu_{23} cluster. The next polyicosahedron is found for Cu_{26} cluster. Finally, the *second* complete icosahedron is formed for Cu_{55} which is more stable than the closed cuboctahedral structure by an energy difference 6.27 eV. This can be explained in terms of their surface energy. The surface energy of the icosahedral structure is lower than that of the cuboctahedral structure, because the atoms on the surface of the icosahedron are five-coordinate compared to the four-coordinate atoms on the surface of the cuboctahedron. In our calculation, exception to the icosahedral growth is found at around Cu_{40} . The situation regarding geometrical structure in this size range is more complex. The structures for $n=40-44$ atom clusters are oblate, decahedronlike geometries. Return to the icosahedral structure is found at $n=45$. In the size range $n=40-44$, the structural sequence is decahedron-icosahedron-cuboctahedron in decreasing order of stability, whereas in the region $n=45-55$, the structures retain icosahedron-decahedron-cuboctahedron sequence.

These results are in agreement with the experimental study of Winter and co-workers [50], where they found that a bare copper cluster mass spectrum recorded with ArF laser ionization shows a sudden decrease in the ion signal at Cu_{42}^+ , and from this observation they argued that a change in geometrical structure might occur there, though they have not concluded about the nature of this geometrical change. They also found a dramatic decrease in water binding energy for Cu_{50} and Cu_{51} , and concluded that this may represent a return to the icosahedral structure as the *second* complete icosahedron is approached for Cu_{55} .

Our prediction agrees with the earlier work by D’Agostino [24], who performed molecular dynamics using a tight-binding many-body potential and found that icosahedral structures are prevalent for clusters containing less than about 1500 atoms. Valkealahti and Manninen [51], using effective medium theory, also found that icosahedral structures are energetically more favorable than the cuboctahedral structures for sizes up to $n \sim 2500$, which is consistent with our result. Figure 3 shows that cuboctahedral structures are least stable among the three structures: icosahedron, decahedron, and cuboctahedron. By contrast, Christensen and Jacobsen [52] predicted more fcc-like structures in the size range $n=3-29$, in their Monte Carlo simulation using an effective medium potential. But they correctly reproduced the “magic numbers” in that regime [52,53].

These results can be compared with the genetic algorithm study on copper clusters by Darby *et al.* [26], using Gupta potential. In agreement with the present study, Darby *et al.* found that most of the clusters in this regime adopt structures based on icosahedron. They also found exceptions to the icosahedral growth at around Cu_{40} , where the structures adopt decahedronlike geometries (exact numbers are not available in Ref. [26]). But the present study disagrees with the genetic algorithm study in two points. First, for the 25-atom cluster, they found a more disordered structure, while the present study predicts it to be an icosahedron based structure which can be derived by removing one surface atom from the 26-atom polyicosahedron. Finally, they found an fcc-like truncated octahedral structure for Cu_{38} . Instead, the present study predicts the icosahedron based structure to be the ground state, where this structure is energetically more favorable than the truncated octahedral structure by an energy $\Delta E=0.17$ eV/atom. Although the genetic algorithm search for global minima is more efficient technique than molecular dynamics, use of the empirical atomistic potential is the main reason [54] for this kind of disagreement between Darby *et al.* and the present study.

B. Binding energies and relative stabilities

The computed size dependence of the binding energy per atom for Cu_n clusters with $n=2-55$ is depicted in Fig. 2 (upper panel). Among all the isomeric geometries examined for a certain cluster size n , the highest cohesive energy has been considered for Fig. 2. The overall shape of the curve matches the anticipated trend: binding energy grows monotonically with increasing the cluster size. Inset of Fig. 2 (upper panel) shows the comparison of our calculated binding energy with the *ab initio* [19,22] and experimental [18] results. Experimentally, the binding energies of the neutral clusters were derived from the dissociation energy data of anionic clusters from the TCID experiment [18] and using electron affinities from the PES experiment [16]. The inset shows that our calculated binding energies are in good agreement with those from DF-LDA [19] and our previous FP-LMTO [22] calculations. However, our binding energies are systematically overestimated, by an energy 0.53 ± 0.12 to 0.79 ± 0.22 , than the experimental binding energies. The LDA-based *ab initio* calculations always overestimate bind-

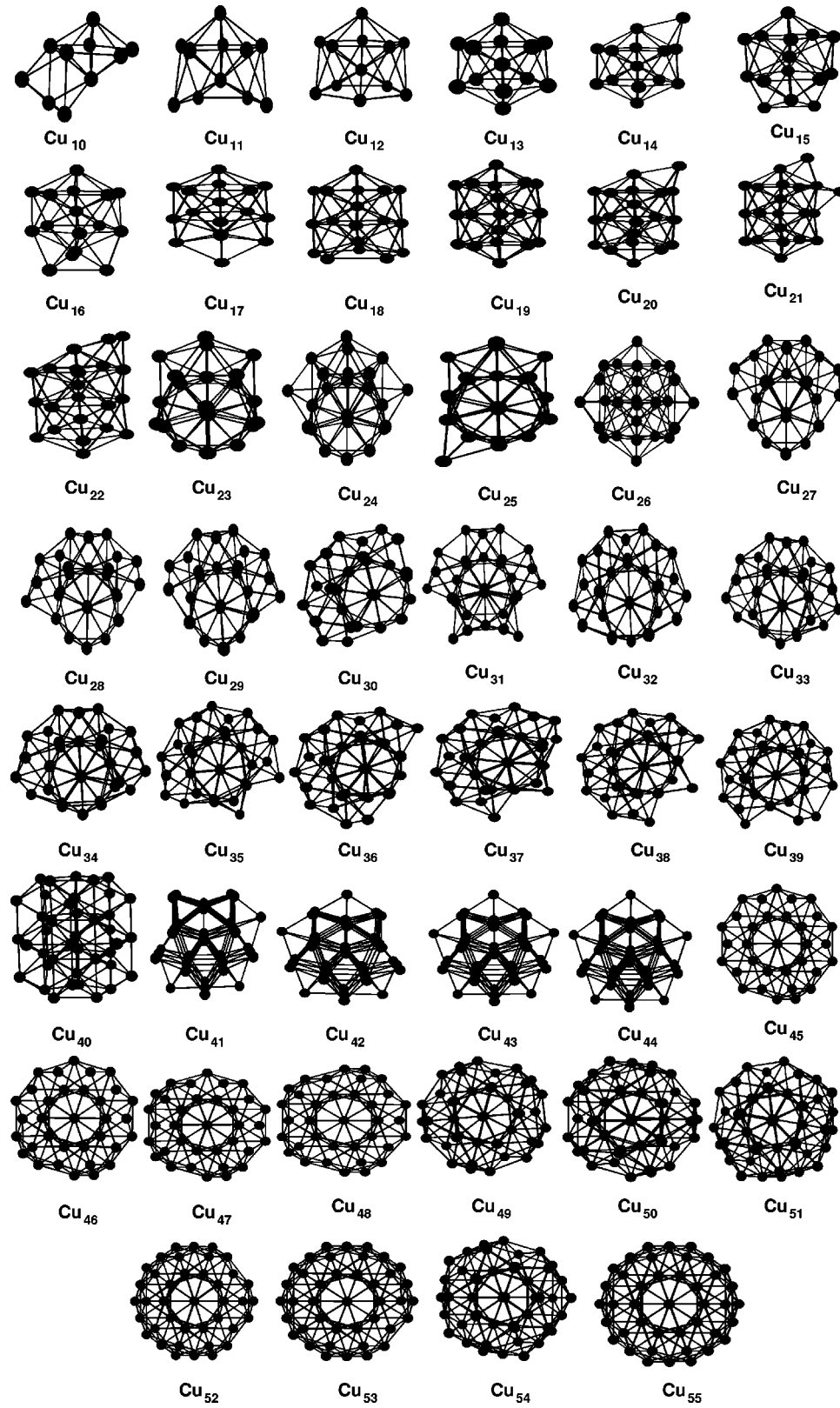


FIG. 1. Most stable structures for copper clusters with $n=10-55$ atoms. Most of the clusters adopt icosahedral structures except for $n=40-44$, where the structures are decahedral.

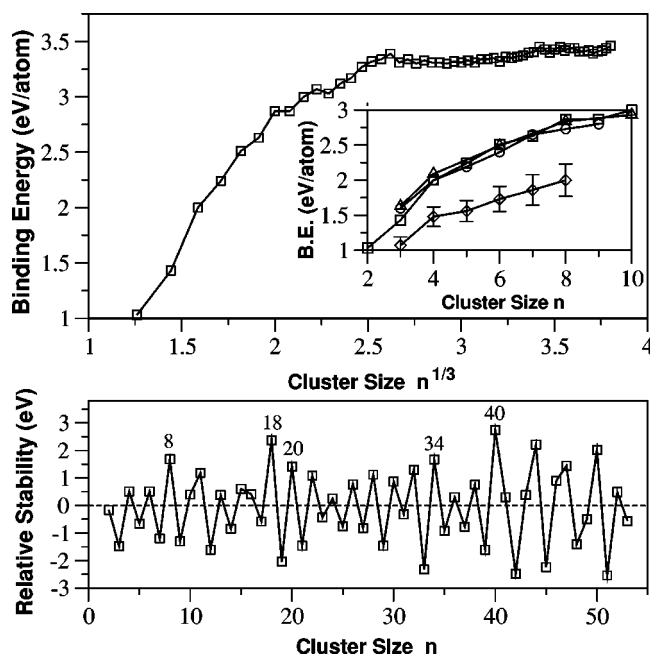


FIG. 2. (Upper panel) Binding energy per atom as a function of cluster size $n^{1/3}$. Inset of the upper panel represents a comparison of binding energy per atom as a function of cluster size n , among the present TBMD (\square), FP-LMTO (\circ), DF-LDA (\triangle) calculations and experimental (\diamond) values. (Lower panel) Variation of relative stability $\Delta_2 E$ with cluster size n . Shell closing effect at $n=8, 18, 20, 34, 40$ and even-odd alternation up to $n \sim 40$ are found. However, due to geometrical effect this even-odd alternation is disturbed at $n=11, 13$, and 15 .

ing energies. This is a characteristic of the LDA. In the present study, TB parameters have been fitted to the *ab initio* LDA calculations for very small calculations [22]. It is not surprising therefore that the binding energies are overestimated. In fact, the present results agree well with other LDA based calculations [19,22], all of which overestimate the binding energy.

In Fig. 3, we compared binding energy per atom for cuboctahedral, decahedral, and icosahedral structures for the clusters containing $n=30-55$ atoms. Figure 3 shows that most clusters in this size range have icosahedral structures. However, a local structural change occurred for $n=40-44$, where the structures adopt a decahedral structure rather than an icosahedral one. Return to the icosahedral growth pattern is found at $n=45$ and continues up to the 55-atom cluster. From Fig. 3 it is clear that among cuboctahedral, decahedral, and icosahedral structures, cuboctahedral structures are least stable than the other two.

The second difference in the binding energy may be calculated as

$$\Delta_2 E(n) = E(n+1) + E(n-1) - 2E(n), \quad (16)$$

where $E(n)$ represents the total energy for an n -atom cluster. $\Delta_2 E(n)$ represents the relative stability of an n -atom cluster with respect to its neighbors and can be directly compared to the experimental relative abundance: the peaks in $\Delta_2 E(n)$ coincide with the discontinuities in the mass spectra. These

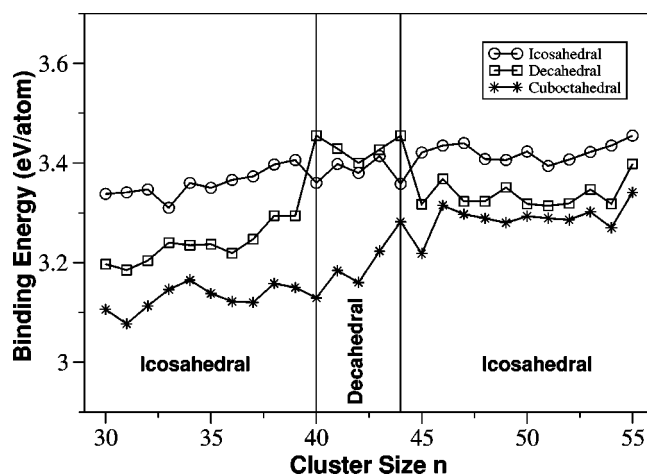


FIG. 3. Comparison of binding energies per atom as a function of cluster size n among cuboctahedral, decahedral, and icosahedral structures. For the whole region most of the clusters prefer icosahedral structure. However, a local geometrical change from icosahedral to decahedral structure is found for $n=40-44$.

are plotted in the lower panel of Fig. 2. We found three major characteristics in Fig. 2 (lower panel). First, even-odd (even $>$ odd) oscillation is found. This can be explained in terms of electron pairing in HOMOs. Even (odd) clusters have an even (odd) number of electrons and the HOMO is doubly (singly) occupied. The electron in a doubly occupied HOMO will feel a stronger effective core potential because the electron screening is weaker for the electrons in the same orbital than for inner shell electrons. Thus the binding energy of the valence electron with an even cluster is larger than of an odd one. This even-odd alternation is prominent up to $n \sim 40$. Second, due to electronic shell or subshell closing, we found particular high peak for $n=8, 18, 20, 34$, and 40 . Unfortunately, the present study does not show any evidence of electronic shell closing for Cu_2 in $\Delta_2 E(n)$. Finally, the even-odd alternation is reversed for $n=10-16$ with maxima at Cu_{11} , Cu_{13} , and Cu_{15} , which manifests the geometrical effect and therefore there is no peak at $n=14$ due to electronic subshell closing. Simultaneous appearance of these three features in $\Delta_2 E(n)$ demonstrates the interplay between electronic and geometrical structure, which is in agreement with the experimental study of Winter *et al.* [50]. They found both jellium like electronic behavior and icosahedral structure in copper clusters. In an experimental study of mass spectra of ionized copper clusters [10], substantial discontinuities in mass spectra at $n=3, 9, 21, 35, 41$ for cationic and $n=7, 19, 33, 39$ for anionic clusters as well as dramatic even-odd alternation are found. From the sudden loss in the even-odd alternation at Cu_{42} in the KrCl spectrum, Winter *et al.* argued about the possible geometrical change there. Therefore, we conclude in the section that sudden loss in the $\Delta_2 E$ versus n plot (lower panel of Fig. 2) is due the structural change in that regime.

Such kind of electronic effects cannot be reproduced by empirical atomistic potentials. Darby *et al.* [26], using the Gupta potential, found significant peaks at $n=7, 13, 19, 23$, and 55 due to icosahedral (or polyicosahedral) geometries. In the present study, we have found a peak at $n=13$, but not at

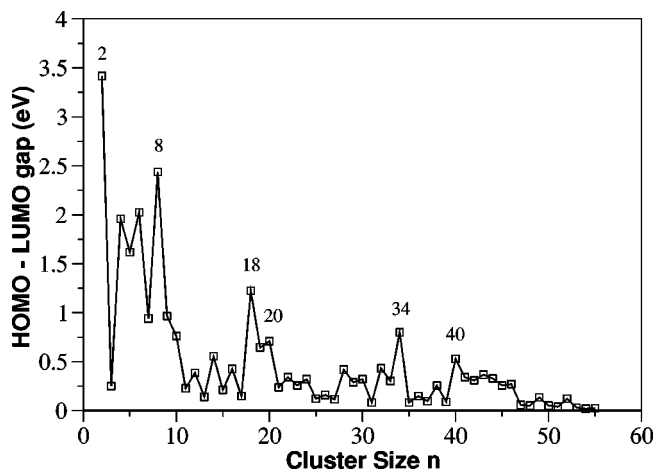


FIG. 4. Highest occupied–lowest unoccupied molecular orbital (HOMO-LUMO) gap energy vs cluster size n . Electronic shell closure at $n=2, 8, 18, 20, 34, 40$ and even-odd alternation are observed. However, sudden loss in even-odd alternation is found around $n \sim 40$ due to the structural change there.

the other sizes found by them. However, the stable structures predicted by us are the same: the lowest energy structure of Cu_7 is a pentagonal bipyramid (D_{5h} symmetry); for $n=13$ and 55, the structures are the *first* and *second* closed icosahedral geometries, respectively. Polyicosahedral structures are found for $n=19$ (double icosahedron) and $n=23$ (triple icosahedron) atom clusters. As a result, the present study shows significant high peaks at Cu_8 , Cu_{18} , and Cu_{20} due to electronic shell closing effect and average peaks at Cu_{22} and Cu_{24} due to electron pairing effect. At these sizes, the electronic effects dominate over the geometrical effects and consequently the above peaks cannot be observed by Darby *et al.*

C. HOMO-LUMO gap energies

Besides the second difference of the cluster binding energy, a sensitive quantity to probe the stability is the HOMO-LUMO gap energy. In the case of magic clusters shell or subshell closure manifests themselves in particularly large HOMO-LUMO gap, which was previously demonstrated experimentally [16,55]. Calculated HOMO-LUMO gap energies are plotted in Fig. 4, where we observed even-odd alternation due to electron pairing effect and particularly large gap for $n=2, 8, 18, 20, 34$, and 40 due to electronic shell and subshell closing. However, sudden loss of even-odd alternation is found around $n \sim 40$ due to the change in the geometrical structure in that region. Winter *et al.* [50] also found a sudden loss in even-odd alternation in the KrCl spectrum at Cu_{42} and concluded that this may coincide with any possible change in the geometrical structure there. In fact, Katakuse *et al.* [10] observed identical behavior in the mass spectra of sputtered copper and silver cluster ions: a dramatic loss of even-odd alternation at $n=42$, signifying a sudden change to a geometrical structure in which stability, and abundance, is less sensitive to electron pairing. Therefore, the sudden loss in Fig. 4 again confirms the structural change there. So, the

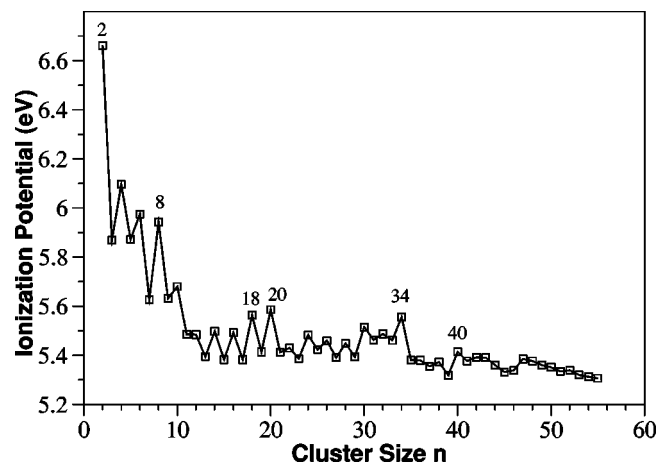


FIG. 5. Ionization potential vs cluster size n . Electronic shell closing effect and prominent even-odd alternation up to $n \sim 40$ are observed.

present study correctly predicts the “magic numbers” in this regime correctly and confirms the experimental prediction: a geometrical change (icosahedron→decahedron) is occurring around $n \sim 40$.

D. Ionization potentials

Within the present TB scheme, we can get a “qualitative” description of the ionization potentials with cluster size according to Koopmans’ theorem. This limitation arises mainly from the choice of the Slater-Koster TB parameters and the extent of their transferability [56], which may be improved by the proposed scaling scheme of Cohen, Mehl, and Papaconstantopoulos [57]. However, our aim is to get only a qualitative description of ionization potential with cluster size. Calculated ionization potentials are plotted in Fig. 5. In fact, we observed the same pattern as in HOMO-LUMO gap energy versus cluster size: peaks at $n=2, 8, 18, 20, 34, 40$ and even-odd alternation due to the same reasons discussed in Sec. III B and III C. Sudden loss in even-odd alternation around $n \sim 40$ is again confirmed from Fig. 5, which is due to the geometrical change there.

IV. CONCLUSION

Using tight-binding model we calculated ground-state geometries, binding energies, second differences in binding energy, HOMO-LUMO gap energies, and ionization potentials for copper clusters in the size range $2 \leq n \leq 55$. We have fitted the parameters of the present TB scheme from our previous *ab initio* calculations [22]. For small clusters $n \leq 9$, present results show good agreement with experimental [16,18] and theoretical [19–22,47–49] results, which allow us to go over the larger size range, $10 \leq n \leq 55$.

In the size range $10 \leq n \leq 55$ most of the clusters adopt icosahedral geometry which can be derived from the 13-atom icosahedron, the polyicosahedral 19-, 23-, and 26-atom clusters, and 55-atom icosahedron, by adding or removing atoms. However, exceptions to the icosahedral growth are found around $n \sim 40$. A local geometrical transition is found

for $n=40-44$ atom clusters. This is in agreement with the prediction of the two experimental studies by Katakuse *et al.* [10] and Winter *et al.* [50], where they predicted that a local geometrical transition may occur at $n=42$, though their results are not decisive about the nature of this geometrical change. Present results show that around $n\sim 40$ structures are changing from icosahedral to decahedral structure, where the structural sequence is decahedron-icosahedron-cuboctahedron in the decreasing order of stability. Return to the icosahedral growth is found at $n=45$, with the sequence icosahedron-decahedron-cuboctahedron in the decreasing order of stability.

As we have fitted the parameters of the present TBMD scheme from LDA based *ab initio* calculations [22], calculated binding energies are in good agreement with the LDA based *ab initio* calculations but overestimate the same calculated from the TCID experiment [18]. In the present scheme, the “magic numbers” ($n=2, 8, 18, 20, 34$, and 40) due to electronic shell and subshell closing are correctly reproduced in the studied regime. Second difference of binding energy, HOMO-LUMO gap energy, and ionization potential show even-odd oscillatory behavior because of electron pairing in

HOMOs in agreement with experiment. However, a sudden loss in even-odd alternation is found around $n\sim 40$ in the variation of second difference in binding energy, HOMO-LUMO gap energy, and ionization potential with cluster size. This is in agreement with the experimental studies [10,50]. We conclude that this is due to the geometrical change (icosahedron \rightarrow decahedron) around there. Present results show that electronic structure can coexist with a fixed atomic packing.

Due to lower computational expense this TBMD scheme, with parameters fitted to first-principle calculation for the smaller clusters and with an environment correction, is a very efficient technique to study larger clusters, particularly with $n\geq 10$.

ACKNOWLEDGMENTS

This work was partially supported by the Centre for Catalytic Systems and Materials Engineering, University of Warwick, U. K. The authors are deeply grateful to S. Mukherjee and Luciano Colombo for a helpful discussion.

-
- [1] W. A. de Heer, Rev. Mod. Phys. **65**, 611 (1993).
 - [2] M. Brack, Rev. Mod. Phys. **65**, 677 (1993).
 - [3] M. Valden, X. Lai, and D. W. Goodman, Science **281**, 1647 (1998).
 - [4] M. B. Kinickelbein, Annu. Rev. Phys. Chem. **50**, 79 (1999).
 - [5] S. H. Joo, S. J. Choi, I. Oh, J. Kwak, Z. Liu, O. Terasaki, and R. Ryoo, Nature (London) **412**, 169 (2001).
 - [6] P. L. Hansen, J. B. Wagner, S. Helveg, J. R. Rostrup-Nielsen, B. S. Clausen, and H. Topsøe, Science **295**, 2053 (2002).
 - [7] C. Binns, Surf. Sci. Rep. **44**, 1 (2001).
 - [8] S. J. Park, T. A. Taton, and C. A. Mirkin, Science **295**, 1503 (2002).
 - [9] D. I. Gittins, D. Bethell, D. J. Schiffrin, and R. J. Nicolas, Nature (London) **408**, 67 (2000).
 - [10] I. Katakuse, T. Ichihara, Y. Fujita, T. Matsuo, T. Sakurai, and H. Matsuda, Int. J. Mass Spectrom. Ion Processes **67**, 229 (1985); **74**, 33 (1986).
 - [11] J. Tiggesbaumer, L. Koller, K. Meiwes-Broer, and A. Liebisch, Phys. Rev. A **48**, R1749 (1993).
 - [12] G. Apai, J. F. Hamilton, J. Stohr, and A. Thompson, Phys. Rev. Lett. **43**, 165 (1979).
 - [13] A. Balerna, E. Bernicri, P. Piccozi, A. Reale, S. Santucci, E. Burrattini, and S. Mobilio, Surf. Sci. **156**, 206 (1985).
 - [14] P. A. Montano, H. Purdum, G. K. Shenoy, T. I. Morrison, and W. Schultze, Surf. Sci. **156**, 216 (1985).
 - [15] K. J. Taylor, C. L. Pettiette-Hall, O. Cheshnovsky, and R. E. Smalley, J. Chem. Phys. **96**, 3319 (1992).
 - [16] J. Ho, K. M. Ervin, and W. C. Lineberger, J. Chem. Phys. **93**, 6987 (1990).
 - [17] M. B. Kinickelbein, Chem. Phys. Lett. **19**, 2129 (1992).
 - [18] V. A. Spasov, T. H. Lee, and K. M. Ervin, J. Chem. Phys. **112**, 1713 (2000).
 - [19] C. Massobrio, A. Pasquarello, and R. Car, Chem. Phys. Lett. **238**, 215 (1995).
 - [20] P. Calaminici, A. M. Köster, N. Russo, and D. R. Salahub, J. Chem. Phys. **105**, 9546 (1996).
 - [21] H. Akeby, I. Panas, L. G. M. Pettersson, P. Seigbahn, and U. Wahlgren, J. Chem. Phys. **94**, 5471 (1990).
 - [22] M. Kabir, A. Mookerjee, R. P. Datta, A. Banerjee, and A. K. Bhattacharya, Int. J. Mod. Phys. B **17**, 2061 (2003).
 - [23] R. P. Datta, A. Banerjee, A. Mookerjee, and A. K. Bhattacharya, *Electronic Structure of Alloys, Surfaces and Clusters*, edited by D. D. Sarma and A. Mookerjee (Taylor and Francis, New York, 2003), p. 348.
 - [24] G. D’Agostino, Philos. Mag. B **68**, 903 (1993).
 - [25] R. P. Gupta, Phys. Rev. B **23**, 6265 (1983).
 - [26] S. Darby, T. V. Mortimer-Jones, R. L. Johnston, and C. Roberts, J. Chem. Phys. **116**, 1536 (2002).
 - [27] M. Menon and R. E. Allen, Phys. Rev. B **33**, 7099 (1986); **38**, 6196 (1988).
 - [28] M. Menon and K. R. Subbaswamy, Phys. Rev. B **47**, 12754 (1993); **50**, 11577 (1994); **51**, 17952 (1996).
 - [29] P. Ordejón, D. Lebedenko, and M. Menon, Phys. Rev. B **50**, 5645 (1994).
 - [30] M. Menon, J. Connolly, N. Lathiotakis, and A. Andriotis, Phys. Rev. B **50**, 8903 (1994).
 - [31] N. Lathiotakis, A. Andriotis, M. Menon, and J. Connolly, J. Chem. Phys. **104**, 992 (1996).
 - [32] J. Zhao, Y. Luo, and G. Wang, Eur. Phys. J. D **14**, 309 (2001).
 - [33] J. C. Slater and G. F. Koster, Phys. Rev. **94**, 1498 (1954).
 - [34] W. A. Harrison, *Electronic Structure and the Properties of Solids* (Dover, New York, 1989).
 - [35] N. Aslund, R. F. Barrow, W. G. Richards, and D. N. Travis, Ark. Fys. **30**, 171 (1965).
 - [36] D. Tomaňek and M. Schluter, Phys. Rev. B **36**, 1208 (1987).
 - [37] K. P. Huber and G. Herzberg, *Molecular Spectra and Molecu-*

- lar Structure* (Van Nostrand-Reinhold, New York, 1989), Vol. IV.
- [38] R. P. Feynman, Phys. Rev. **56**, 340 (1939).
 - [39] L. Colombo (unpublished).
 - [40] W. C. Swope, H. C. Anderson, P. H. Berenes, and K. R. Wilson, J. Chem. Phys. **76**, 637 (1982).
 - [41] M. S. Methfessel and M. van Schilfgaarde, Phys. Rev. B **48**, 4937 (1993); , Int. J. Mod. Phys. B **7**, 262 (1993); M. Methfessel, M. van Schilfgaarde, and M. Scheffler, Phys. Rev. Lett. **70**, 29 (1993).
 - [42] D. M. Deaven and K. M. Ho, Phys. Rev. Lett. **75**, 288 (1995); D. M. Deaven, N. Tit, J. R. Morris, and K. M. Ho, Chem. Phys. Lett. **256**, 195 (1996).
 - [43] B. Hartke, Chem. Phys. Lett. **240**, 560 (1995).
 - [44] Y. H. Luo, J. J. Zhao, S. T. Qiu, and G. H. Wang, Phys. Rev. B **59**, 14903 (1999).
 - [45] J. A. Niese and H. R. Mayne, Chem. Phys. Lett. **261**, 576 (1996); J. Chem. Phys. **105**, 4700 (1996).
 - [46] M. Kabir, A. Mookerjee, and A. K. Bhattacharya (unpublished).
 - [47] C. W. Bauschlicher, Jr., S. R. Langhoff, and H. Partridge, J. Chem. Phys. **91**, 2412 (1989); C. W. Bauschlicher, Jr., Chem. Phys. Lett. **156**, 91 (1989).
 - [48] U. Lammers and G. Borstel, Phys. Rev. B **49**, 17360 (1994).
 - [49] Y. Wang, T. F. George, D. M. Lindsay, and A. C. Beri, J. Chem. Phys. **86**, 3593 (1987); D. M. Lindsay, L. Chu, Y. Wang, and T. F. George, *ibid.* **87**, 1685 (1987).
 - [50] B. J. Winter, E. K. Parks, and S. J. Riley, J. Chem. Phys. **94**, 8618 (1991).
 - [51] S. Valkealahti and M. Manninen, Phys. Rev. B **45**, 9459 (1992).
 - [52] O. B. Christensen and K. W. Jacobsen, J. Phys.: Condens. Matter **5**, 5591 (1993).
 - [53] O. B. Christensen, K. W. Jacobsen, J. K. Norskov, and M. Manninen, Phys. Rev. Lett. **66**, 2219 (1991).
 - [54] Even a small variation in the parameters (in particular, parameter q) in the Gupta potential can lead to changes in the global minima. See K. Michaelian, N. Rendon, and I. L. Garzón, Phys. Rev. B **60**, 2000 (1999).
 - [55] C. L. Pettiette, S. H. Yang, M. J. Craycraft, J. Conceicao, R. T. Laaksonen, O. Cheshnovsky, and R. E. Smalley, J. Chem. Phys. **88**, 5377 (1988).
 - [56] The set of SK-TB parameters in this scheme implies that within the Koopmans' theorem, ionization potentials are approximately equal to the on-site energy $E_s=E_d$, which is usually much higher than highest-occupied s -orbital energy of the free atom. A constant shift is made in plotting of Fig. 5. See Ref. [31].
 - [57] R. E. Cohen, M. J. Mehl, and D. A. Papaconstantopoulos, Phys. Rev. B **50**, 14694 (1994).